SUPPLEMENTARY INFORMATION

Fluorescence Spectroscopy Studies of Crossed Aldol Reactions: A Reactive Nile Red Dye Reveals Catalyst-Dependent Product Formation

Judith Bautista-Gomez,[†] Abdulhafiz Usman,[‡] Man Zhang,[†] Ryan J. Rafferty,[†] Stefan H. Bossmann,[†] Keith L. Hohn,[,‡] and Daniel A. Higgins*[,†]*

[†]Department of Chemistry and [‡]Department of Chemical Engineering, Kansas State University, Manhattan, Kansas 66506, United States

Additional data showing the characterization of the two catalysts employed, Cs(Mg,Zr)-SiO_2, and MgO, as well as fumed silica (SiO_2) are provided. The data show nitrogen adsorption and desorption isotherms and mesopore size distributions **(Figure S1)**, XPS spectra **(Figure S2)**, and CO_2 and NH_3 temperature programmed desorption curves **(Figure S3).** Data showing fluorescence spectra of NR-CHO compared to commercial Nile Red **(Figure S4)** are also given. MS data from aldol products produced in 3-day reactions of NR-CHO with acetone and acetophenone on Cs(Mg,Zr)-SiO_2 and MgO catalysts are included **(Figure S5)**. The stability of NR-CHO in contact with the active heterogeneous catalysts is investigated **(Figure S6)**. Fluorescence spectra of the pure aldol products from NR-CHO reactions with acetone or acetophenone are provided **(Figure S7)**. HPLC chromatograms were also obtained to show the ratio of aldol products produced in reactions employing Cs(Mg,Zr)-SiO_2 catalysts **(Figure S8)**. Finally, additional data showing results from similar aldol reactions run with commercially available 3-perylene carboxaldehyde are provided. The data show the static fluorescence spectra of the dye in DMSO **(Figure S9)**, as well as fluorescence spectra of aldol reactions comparing Cs(Mg,Zr)-SiO_2 and MgO catalysts **(Figure S10)**.

Corresponding author email:

[‡]Hohn@ksu.edu
[†]Higgins@ksu.edu

Nitrogen Sorption Isotherms

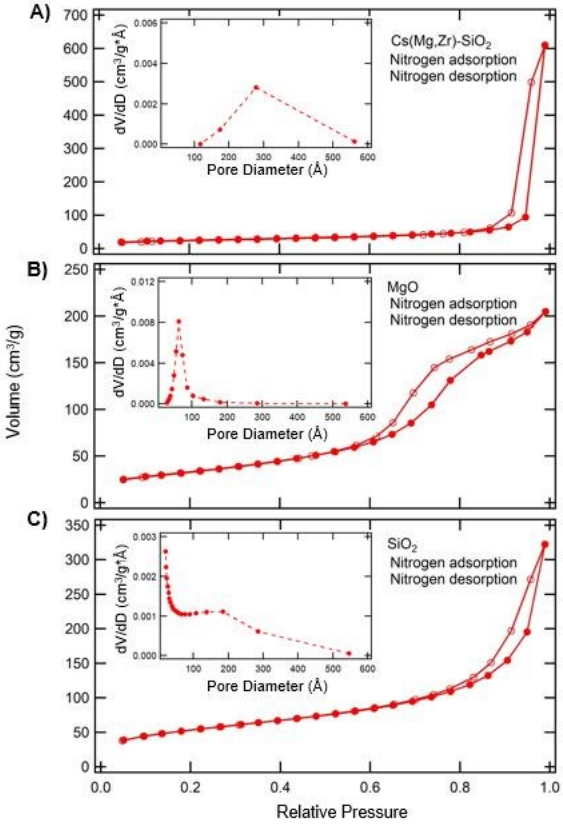

Figure S1. Nitrogen adsorption (filled circles) and desorption (open circles) isotherms of mesoporous catalysts Cs(Mg,Zr)-SiO_2 **(A)**, MgO **(B)**, and fumed silica **(C)**. The insets denote the pore-size distribution of each and were obtained from the respective desorption isotherm.

Catalyst Composition

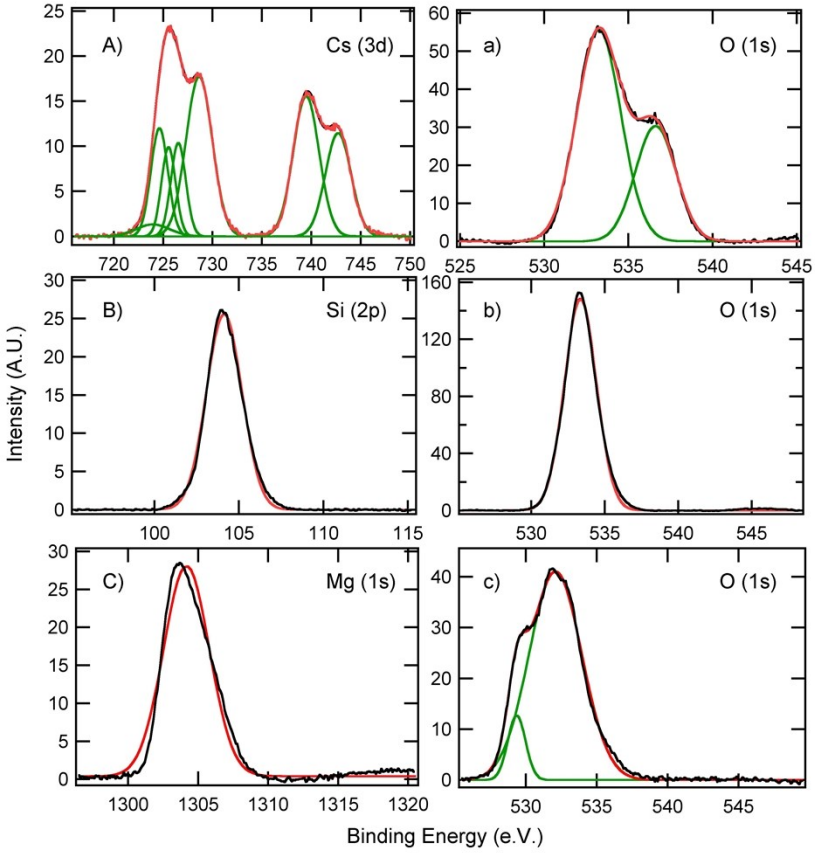

Figure S2. XPS spectra of the Cs(Mg,Zr)-SiO_2 catalyst. The Cs (3d) spectrum **(A)** includes peaks at 725.6 and 739.8 eV corresponding to Cs $3d_{5/2}$ and Cs $3d_{3/2}$ from the Cs^+ ion.[1] The peaks at 724.6 eV, 725.5 eV are attributed to Cs_2O_2,[2] and Cs_2O,[3] while those at > 726 eV are attributed to suboxides of Cs.[4] The O (1s) spectrum **(a)** includes a peak at 533.2 eV due to Si-O (Si-O-Si, Si-O-H) from the SiO_2 support.[5] XPS spectra of SiO_2 **(B)** reveal the Si (2p) peak at 104.1 eV due to Si-O_2,[6] while its O (1s) spectrum **(b)** gives a peak 533.2 eV due to Si-O (Si-O-Si, Si-O-H) from the SiO_2 support.[5] XPS spectra of the MgO catalyst **(C)** include the Mg (1s) peak at 1304.2 eV due to Mg-O,[7] with its O (1s) spectrum **(c)** incorporating a peak at 529.4 eV attributable to lattice oxygen O^{2-}. The higher binding energy peak at 532.0 eV can be attributed to adsorbed oxygen, weakly bound oxygen, or to surface hydroxyl species.[8-9]

Catalyst Basicity and Acidity

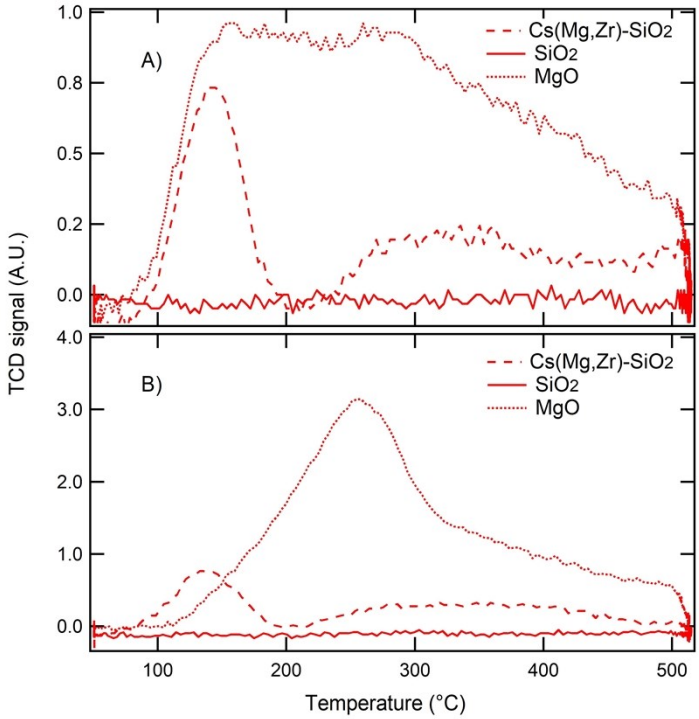

Figure S3. (A) CO_2 and **(B)** NH_3 temperature programmed desorption curves of Cs(Mg,Zr)-SiO_2, SiO_2 and MgO catalysts. Higher desorption temperatures indicate stronger basicity or acidity while the area under the desorption peaks provides the number of active sites.[10] The desorption profile for SiO_2 showed no detectable basic or acid sites. The CO_2 desorption profile for Cs(Mg,Zr)-SiO_2 showed two prominent peaks at 75-175°C (weak strength basic sites) and 275-475°C (medium strength basic sites) while for MgO, a broad CO_2 desorption peak at 75-475°C (weak-medium strength sites) was observed. The NH_3 desorption profile for Cs(Mg,Zr)-SiO_2 also showed peaks at 75-175°C (weak strength acid sites) and at 250-475°C (medium strength acid sites). The commercial MgO catalyst showed a prominent desorption peak at 200-300°C, corresponding to medium strength acid sites.

NR and NR-CHO Fluorescence Spectra

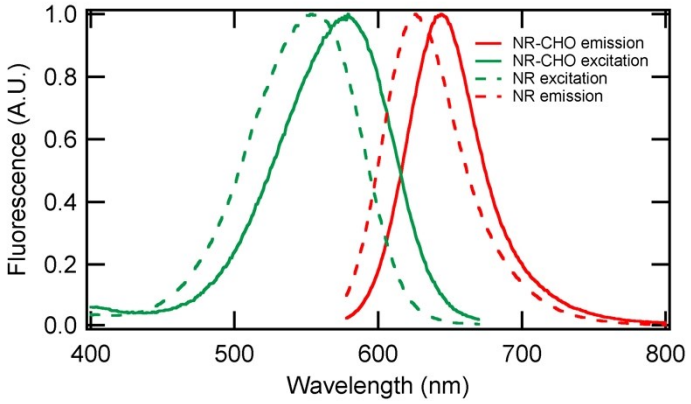

Figure S4. Normalized fluorescence excitation (green) and emission (red) spectra of 1 μM commercial Nile Red (NR) and 1 μM (NR-CHO) in DMSO. The absorbance and emission spectra of the newly synthesized derivative of Nile Red are shifted ~24 nm and ~18 nm respectively to longer wavelengths compared to the commercial Nile Red.

Aldol Reaction Product Mass Spectra

Aldol Reactions Catalyzed by $Cs(Mg,Zr)-SiO_2$

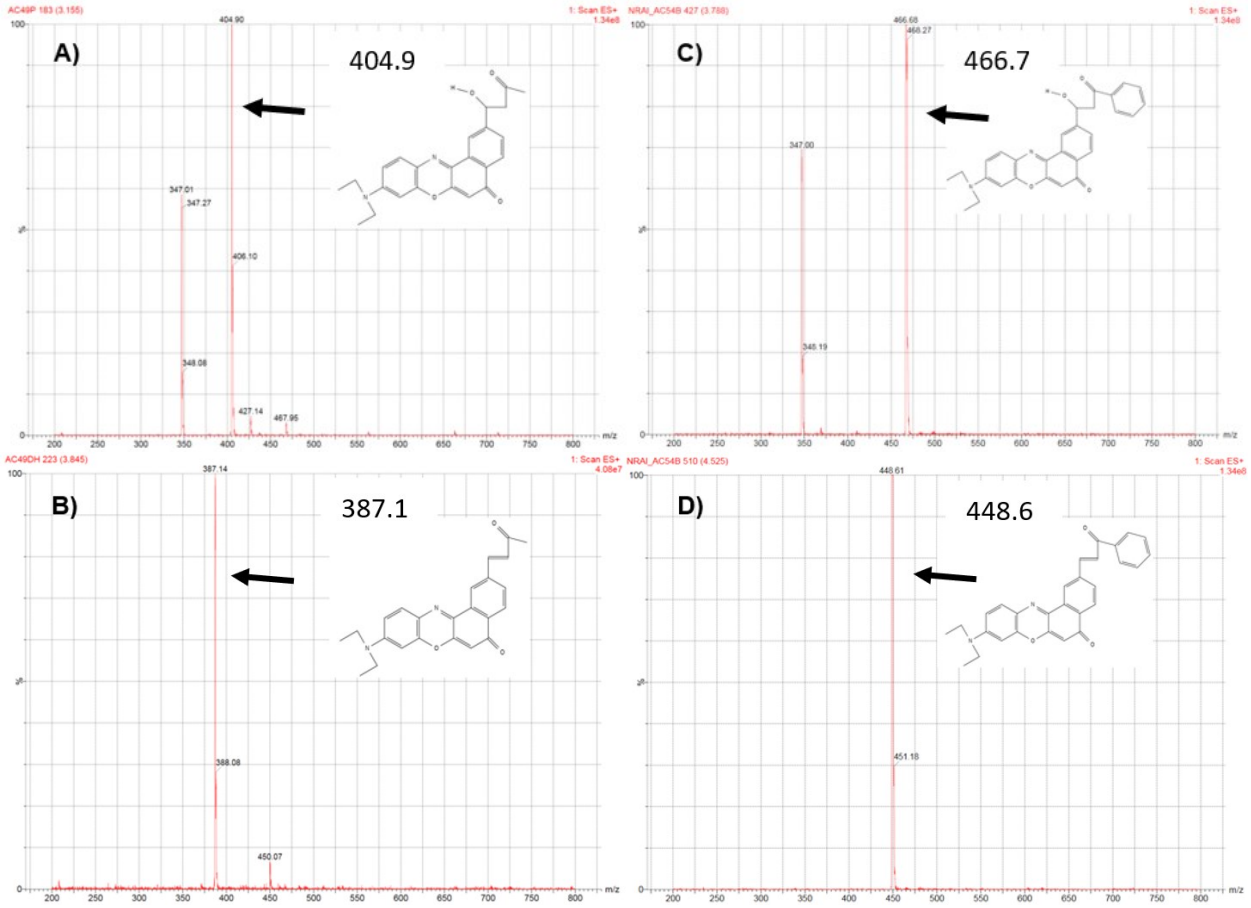

Aldol Reactions Catalyzed by MgO

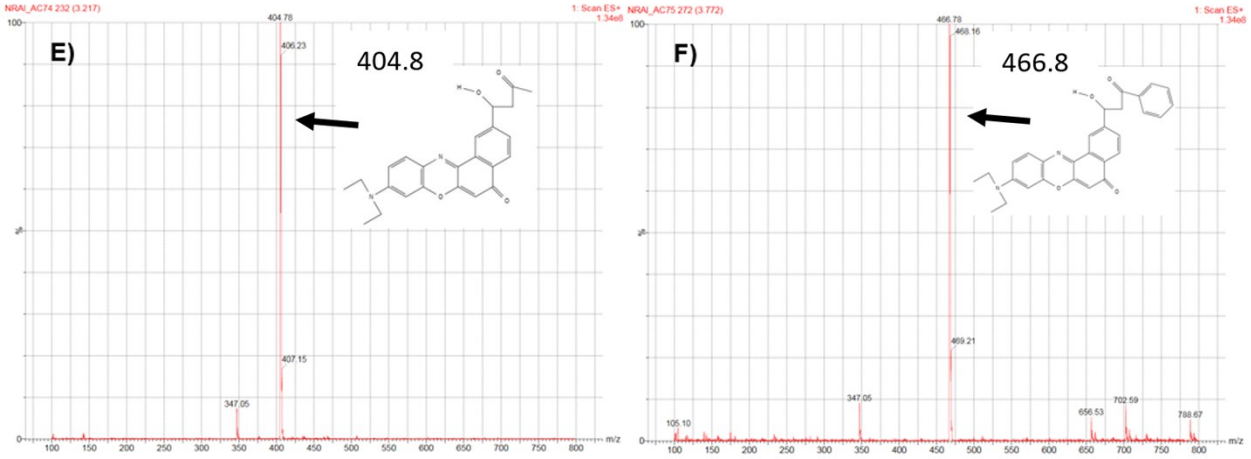

Figure S5 HPLC-MS data from aldol addition and condensation products obtained after 3-day reactions of **(A, B)** NR-CHO with acetone and **(C, D)** NR-CHO with acetophenone using the Cs(Mg,Zr)-SiO_2 catalyst. **(A)** Aldol addition product, 405 amu; **(B)** aldol condensation product, 387 amu; **(C)** aldol addition product, 467 amu; **(D)** aldol condensation product, 449 amu. HPLC-MS of aldol addition products from 3-day reactions of **(E)** NR-CHO with acetone and **(F)** NR-CHO with acetophenone using the MgO catalyst. **(E)** aldol addition product, 405 amu; **(F)** aldol addition product, 467 amu. The molecules were ionized by electrospray ionization.

NR-CHO Stability in Active Heterogeneous Catalysts

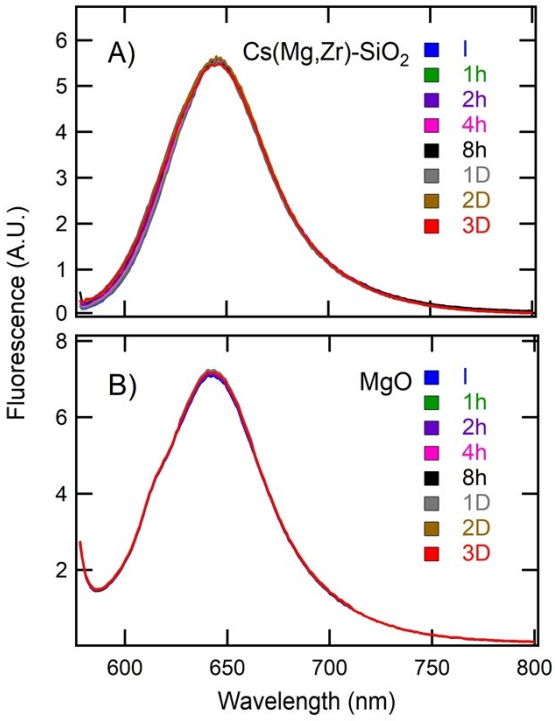

Figure S6 NR-CHO (1 μM) stability in the presence of active heterogeneous catalysts **A)** Cs(Mg,Zr)-SiO_2, and **B)** MgO. These experiments were run under identical conditions to those described in the main text, with the one exception that no ketone was added to the reaction mixture. Fluorescence was excited at 575 nm in each case. DMSO was employed as the solvent. All reactions were stirred at room temperature.

Spectra of Pure Aldol Products

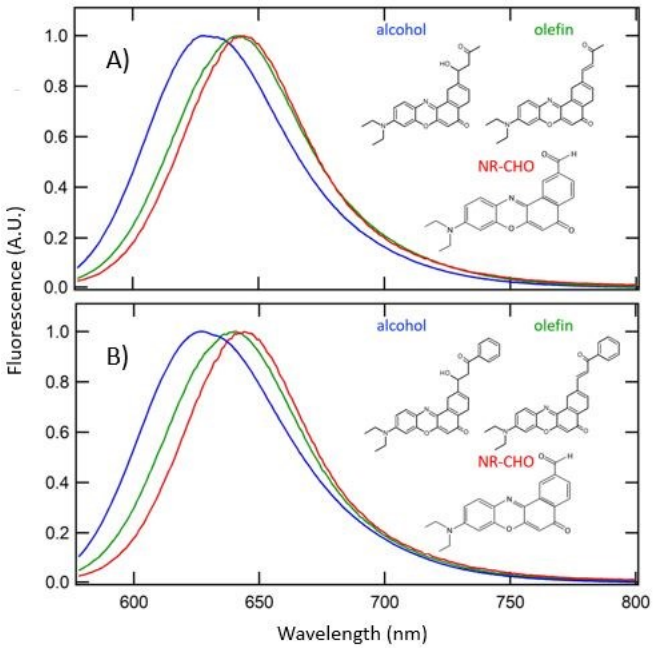

Figure S7 A) Normalized fluorescence emission spectra of 1 μM NR-CHO (red), products from NR-CHO-acetone aldol reaction: alcohol (blue), and olefin (green) in DMSO. **B)** Normalized fluorescence emission spectra of 1 μM NR-CHO (red), products from NR-CHO-acetophenone aldol reaction: alcohol (blue), and olefin (green) in DMSO. The emission spectra of the alcohol and olefin products in both aldol reactions are shifted ~13 nm and ~2-4 nm respectively to shorter wavelengths compared to NR-CHO.

Aldol Reaction Kinetics and Product Formation

Based on kinetic data from Figures 6A, D in the main text, it appears the Cs(Mg,Zr)-SiO_2 catalyzed reactions with acetone and acetophenone were nearly complete at ~ 2 h and ~ 12 h, respectively. Analytical HPLC was again used to confirm completeness of the reactions and to further characterize the products formed. These reactions were again run at high NR-CHO concentration (1 mM) and under identical reaction conditions to those described in the main text. Product mixtures obtained from the acetone and acetophenone reactions after arbitrarily selected

times of 8 h and 17 h, respectively, were compared to those obtained after 3 days. The HPLC data showed that the product mixtures obtained from the acetone reaction after 8h and 3 days were very similar. Figures S7A, B show these results. Only a small amount of NR-CHO remained after 8h and that amount was significantly lower after 3 days. Greater conversion of the aldol addition product to the condensation product was also observed after 3 days. The acetophenone reaction was once again found to be much slower. Figures S7C, D show that after 17 h, a significant amount NR-CHO remained in the mixture. After 3 days, more NR-CHO had been converted to the aldol addition product. However, the longer reaction time did not appear to result in higher conversion of aldol addition product to the condensation product. It is uncertain why more condensation product was not found in the reaction mixture after 3 days.

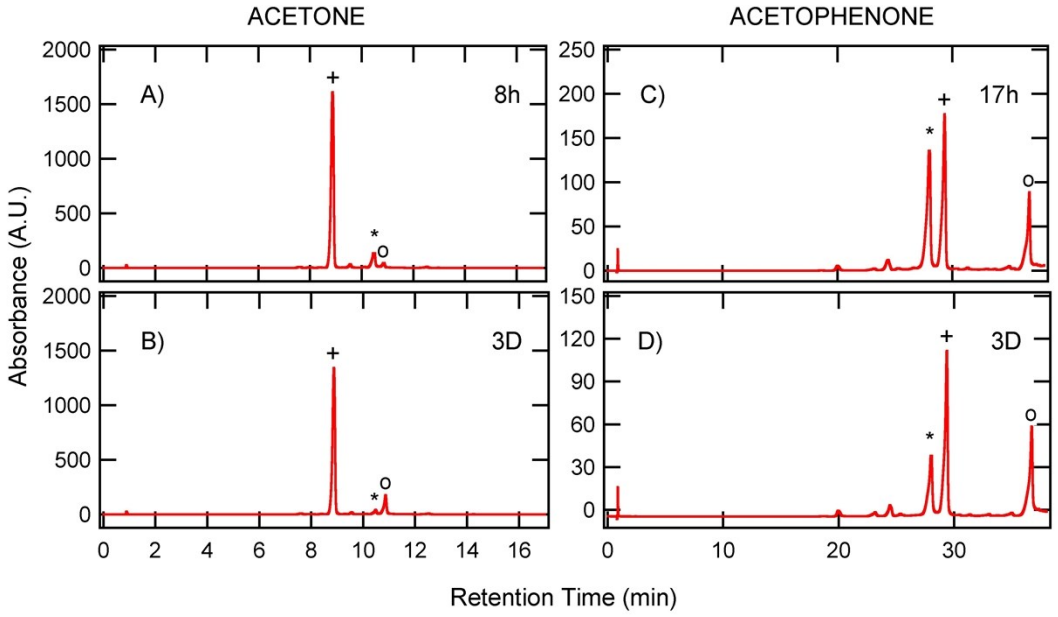

Figure S8. HPLC chromatograms (575 nm absorbance) of aldol products for the NR-CHO (1mM) reaction with acetone at 8h and 3 days **(A, B)**, and acetophenone at 17h and 3 days **(C, D)** in the presence of Cs(Mg,Zr)-SiO_2 at room temperature. The chromatograms show unreacted NR-CHO **(*)**, the aldol addition product **(+)**, and the aldol condensation product **(o)**. Aldol reactions at 8h and 17h had a higher amount of unreacted NR-CHO than 3-day reactions. The peak area ratio of unreacted NR-CHO to aldol condensation product was ~ 4 and ~ 1.5 for acetone and acetophenone 8h and 17h reactions, respectively. While that peak area ratio was ~

0.2 and ~ 0.8 for acetone and acetophenone 3-day reactions, respectively. Note that aldol reactions with acetone are faster than those with acetophenone, likely due to the greater number of acidic hydrogens on the former. Allowing the NR-CHO-acetone reaction to run for 3 days yielded a higher conversion of aldol addition to aldol condensation products, yielding peak area ratios of ~ 31 and ~ 7 in 8h and 3-day reactions, respectively. However, in the NR-CHO-acetophenone reaction, the peak area ratio of aldol addition to aldol condensation products remained the same (~2) even after 3-days. Note that the peak area ratio of unreacted NR-CHO to aldol addition product was lower after 3-days (i.e., ~ 0.5 compared to ~ 0.8 in the 17h reaction). For **A, B,** the mobile phase gradient comprised H_2O and acetonitrile mixtures at 0.800 mL/min flow rate with the following compositions: 0-10 min: 95-40% H_2O; 10-15 min: 40-20% H_2O; 15-17 min: 20% H_2O. For **C, D** the mobile phase compositions were: 0-35 min: 95-45% H_2O; 35-36 min: 45-20% H_2O; 36-38 min: 20% H_2O. A Thermo Scientific Hypersil GOLD C18 column (100 X 3 mm^2, 3 μm particle size) was employed.

3-Perylenecarboxaldehyde Fluorescence Spectra and Aldol Reaction Results

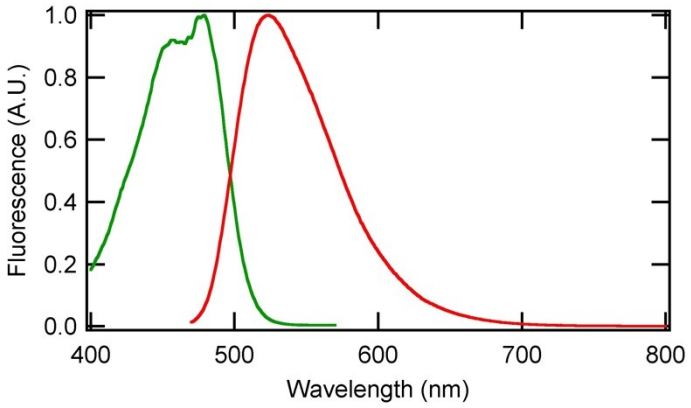

Figure S9. Normalized fluorescence excitation (green) and emission (red) spectra of 1 μM 3-perylenecarboxaldehyde in DMSO. The excitation spectrum is peaked at 476 nm with a vibronic band appearing at 456 nm. The emission spectrum is centered at 523 nm.

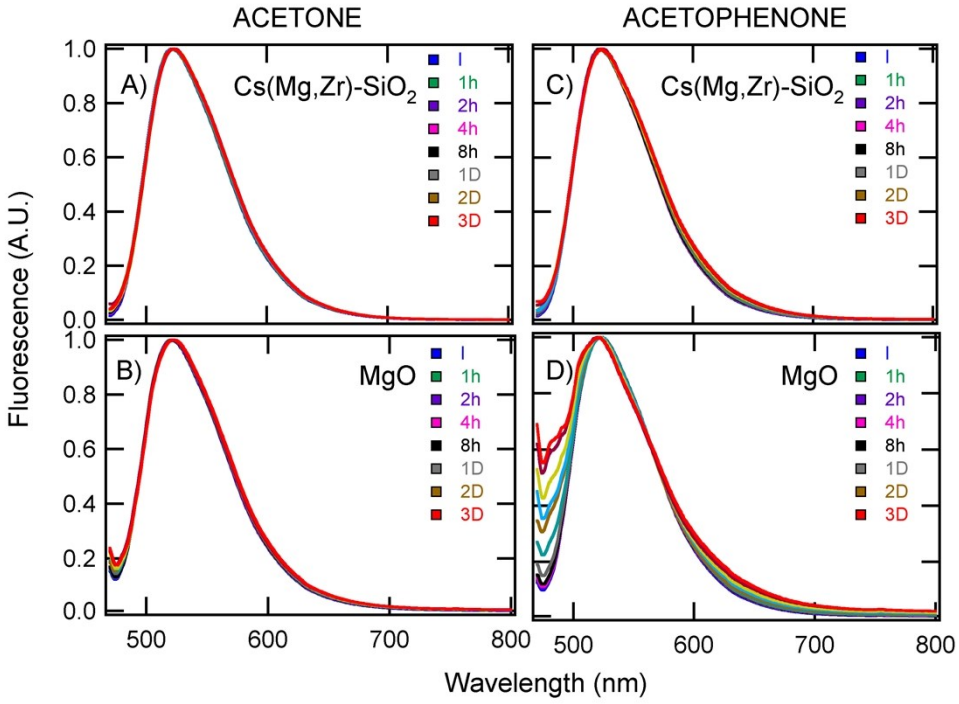

Figure S10. A), B) Fluorescence from 3-perylenecarboxaldehyde as a function of time in the presence of the catalysts listed with acetone employed as the ketone. **C), D)** Fluorescence from 3-perylenecarboxaldehyde as a function of time in the presence of the catalysts listed with acetophenone employed as the ketone. The fluorescence was excited at 465 nm in each

experiment. DMSO was employed as the solvent. All reactions were stirred at room temperature. Aldol reactions with acetone yielded nearly identical fluorescence spectra for the two different catalysts. While aldol reactions of the dye with acetophenone and MgO catalyst gave slightly different fluorescence spectra where it appeared that a very small shoulder centered at ~ 480 nm arose after 2 days. In contrast, very distinct fluorescence spectra were observed after only a few hours in aldol reactions with the reactive NR-CHO dye and the same catalysts, Figure 4 in the main text. MS data provided support for the formation of aldol products under the above experimental conditions in reactions employing a higher concentration of 3-perylenecarboxaldehyde (1 mM), data not shown.

References

1. Podgornov, E. A.; Prosvirin, I. P.; Bukhtiyarov, V. I. XPS, TPD and TPR Studies of Cs-O Complexes on Silver: Their Role in Ethylene Epoxidation. *J. Mol. Catal. A-Chem* **2000,** *158*, 337-343.
2. van der Heide, P. A. W. Cesium-Induced Transient Effects on the Si+ and Si-Secondary Ion Emissions from Si and SiO_2. *Surf. Sci.* **2000,** *447*, 62-72.
3. Phillips, C. C.; Hughes, A. E.; Sibbett, W. Quantitative XPS Surface Chemical Analysis and Direct Measurement of the Temporal Response Times of Glass-Bonded NEA GaAs Transmission Photocathodes. *J. Phys. D. Appl. Phys.* **1984,** *17*, 1713-1725.
4. Ebbinghaus, G.; Simon, A. Electronic Structures of Rb, Cs and Some of Their Metallic Oxides Studied by Photoelectron Spectroscopy. *Chem. Phys.* **1979,** *43*, 117-133.
5. Beketov, G.; Heinrichs, B.; Pirard, J. P.; Chenakin, S.; Kruse, N. XPS Structural Characterization of Pd/SiO_2 Catalysts Prepared by Cogelation. *Appl. Surf. Sci.* **2013,** *287*, 293-298.
6. Arezzo, F.; Severini, E.; Zacchetti, N. An XPS Study of Diamond Films Grown on Differently Pretreated Silicon Substrates. *Surf. Interf. Anal.* **1994,** *22*, 218-223.
7. Wu, M. Z.; Fu, Y.; Zhan, W. C.; Guo, Y. L.; Guo, Y.; Wang, Y. S.; Lu, G. Z. Catalytic Performance of MgO-Supported Co Catalyst for the Liquid Phase Oxidation of Cyclohexane with Molecular Oxygen. *Catalysts* **2017,** *7*, 155.
8. Wang, X. Y.; Kang, Q.; Li, D. Low-Temperature Catalytic Combustion of Chlorobenzene Over MnO_x-CeO_2 Mixed Oxide Catalysts. *Catal. Commun.* **2008,** *9*, 2158-2162.
9. Yao, H. C.; Yao, Y. F. Y. Ceria in Automotive Exhaust Catalysts: I. Oxygen Storage. *J. Catal.* **1984,** *86*, 254-265.
10. Faba, L.; Diaz, E.; Ordonez, S. Aqueous-Phase Furfural-Acetone Aldol Condensation Over Basic Mixed Oxides. *Appl. Catal. B-Environ.* **2012,** *113*, 201-211.